

## Real-time recovery of the electron density from interferometric measurements affected by fringe jumps

A. Murari, L. Zabeo, A. Boboc, D. Mazon, and M. Riva

Citation: [Review of Scientific Instruments](#) **77**, 073505 (2006); doi: 10.1063/1.2219731

View online: <https://doi.org/10.1063/1.2219731>

View Table of Contents: <http://aip.scitation.org/toc/rsi/77/7>

Published by the [American Institute of Physics](#)

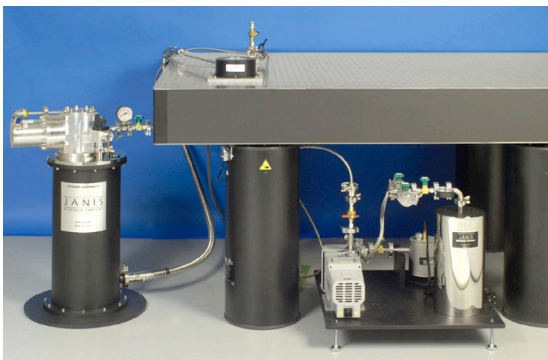
---

### Articles you may be interested in

[JET polari-interferometer](#)

[Review of Scientific Instruments](#) **60**, 2825 (1989); 10.1063/1.1140666

---



# JANIS

**Rising LHe costs? Janis has a solution.**  
Janis' Recirculating Cryocooler eliminates the use of Liquid Helium for "wet" cryogenic systems.

[sales@janis.com](mailto:sales@janis.com) [www.janis.com](http://www.janis.com) **Click for more information.**

## Real-time recovery of the electron density from interferometric measurements affected by fringe jumps

A. Murari

*Consorzio RFX Associazione EURATOM-ENEA per la Fusione, C.so Stati Uniti 4, 35127, Padova, Italy*

L. Zabeo and A. Boboc<sup>a)</sup>

*EURATOM/UKAEA Fusion Association, Culham Science Centre, Abingdon, OX14 3DB, United Kingdom*

D. Mazon

*Association EURATOM-CEA, CEA Cadarache, F-13108, St Paul lez Durance, France*

M. Riva

*Associazione EURATOM-ENEA sulla Fusione, C.R. Frascati, 00044 Frascati, Italy*

(Received 11 April 2006; accepted 5 June 2006; published online 21 July 2006)

Optical interferometers are normally used in magnetically confined plasmas to measure the refractive index of the plasma by comparing the phase shift variation between a reference and a probe laser beam, from which the line-integrated electron density can be derived. Unfortunately, interferometric measurements are affected by fringe jumps, which are basically the erroneous phase difference determination due to the loss of signals or a phase difference bigger than  $2\pi$ . The multiple causes include the refraction, wavelength of the laser radiation used, sensitivity, and time resolution of the measurements. On the other hand, the plasma density has become an essential piece of information for many real-time control schemes, which can therefore be completely jeopardized by fringe jumps. To overcome this problem at JET two main approaches can be adopted. The first approach consists of performing a real-time correction of the affected chords, eliminating the spurious effect of the fringe jumps, and providing a corrected line integral of acceptable quality. This is done at JET by complex algorithms that have inputs of various interferometry and polarimetry measurements. A second approach can be adopted based on the observation that, for many real-time experiments, an approximate estimate of the density profile is sufficient. In JET, it was demonstrated that the density profile of the vast majority of configurations could be determined with sufficient accuracy by using only the line-integrated density profile provided by two chords; one external and one internal. The various solutions were tested and results compared in order to verify the most suitable one for the various plasma configurations and operational scenarios. A “general purpose” version of the correction algorithm was implemented and is now normally running during JET operation. © 2006 American Institute of Physics. [DOI: [10.1063/1.2219731](https://doi.org/10.1063/1.2219731)]

### I. INTRODUCTION

In general, interferometers measure the optical path along a light beam in terms of the radiation wavelength.<sup>1</sup> The optical path is the product of the geometrical path and the refractive index of the medium. In magnetically confined plasmas, which are very difficult to access and diagnose, interferometry is a very powerful tool to determine the refractive index and derive from it the plasma density.

Long wavelengths are less prone to vibration effects where the shorter allow better resolution of the measurements. Far-infrared wavelengths are the best compromise if we introduce the problem of the absorption/refraction inside the plasma. To compensate for the possible variations of the optical path, a second compensation laser is often installed; implementing so-called two-color interferometers. Unfortu-

nately, laser beams with longer wavelengths are also more strongly refracted due to plasma density gradients that cause variations of the refractive index.

In fusion machines abrupt transient changes of the density gradient of the plasma, and therefore of the refractive index, can be the consequence of both plasma phenomena, such as, edge localized modes (ELMs) or disruptions. These phenomena significantly degrade the signals. Moreover, externally triggered events, such as pellet injection, cause a phase variation of the beam, which is faster than the modulation frequency introducing uncertainty on the measurements. All of these particular events that affect the correct measurement of the plasma density are called fringe jumps (see Sec. II). In the last years, the real-time control of various plasma scenarios has become one of the most qualifying programs on the route to a next step Tokamak. The feasibility of these control schemes crucially depends on the quality and reliability of the diagnostics involved, and the plasma density is one of the most frequently required. In this perspective, on JET, a fast acquisition system<sup>2</sup> for the interferometer/

<sup>a)</sup>Electronic mail: alexandru.boboc@jet.efda.org

polarimeter diagnostic<sup>3</sup> was recently installed (see Sec. II). It produces a measurement every millisecond, and it was fully validated in the last campaigns. The main problem faced by the system consists of the fringe jumps; a consequence of the strong variations of the density, which can completely jeopardize several real-time control schemes. In this article, a quite exhaustive series of techniques to recover the correct measurement of the electron density after a fringe jump is reviewed and the results of their implementation on JET are reported.

In general, two main approaches can be adopted; one meant to correct the effect of the fringe jumps and recover the correct line integrated signals, and the second aiming at the derivation of an approximated density profile on the basis of a minimum number of chords available. In the first approach, the possible methods—which can be used to correct the interferometric measurements after the occurrence of fringe jumps—fall mainly in two groups. The first category includes the approaches that use only the interferometric data (see Sec. III). The most effective correction algorithm in this class exploits the two colors of the lateral channels. The signals of the two lasers are compared, and this allows identifying the most suitable correction of the measurements. In the case of the vertical channels, for which the second color is not available, one reasonable alternative—very useful for the high time resolution that it guarantees—is based on the comparison of the chord affected by the fringe jump with the closest lateral line of sight. By taking into account, the relative length of the chords—available in real time—and a suitable profile factor, the proper value of the measurement can be recovered. A possible different approach consists of reconstructing the entire density profile, with only the chords not affected by the fringe jumps or the horizontal ones corrected using the second color, and then calculating the missing line integrals.

The second class of solutions includes methods based on the effect of an optically active medium, such as fusion plasmas, on the plane of polarization of the beam light. The two essential physical phenomena investigated so far are the Faraday rotation and Cotton-Mouton effect (see Sec. IV). The polarization plane of a laser beam is rotated by magnetized plasma of an angle, which depends on the product of the electron density and the magnetic field parallel to the propagation direction. This so-called Faraday rotation can be exploited in a machine, such as JET, to determine the plasma density at the edge of the plasma column, where the magnetic field is known from the external pick up coils (see Sec. IV). The Faraday rotation is indeed normally well below 360° and therefore the loss of the signal for short intervals—due to ELMs or pellets—does not compromise the measurement.

This is also because it is an absolute measurement and not history dependent, such as in the case of interferometric measurements. This solution is particularly useful for the correction of the external channels during pellet injections, which have such a strong effect on the plasma to sometime compromise the other techniques. The Cotton-Mouton effect consists of the change of ellipticity of the radiation propagating perpendicular to a component of the magnetic field (see

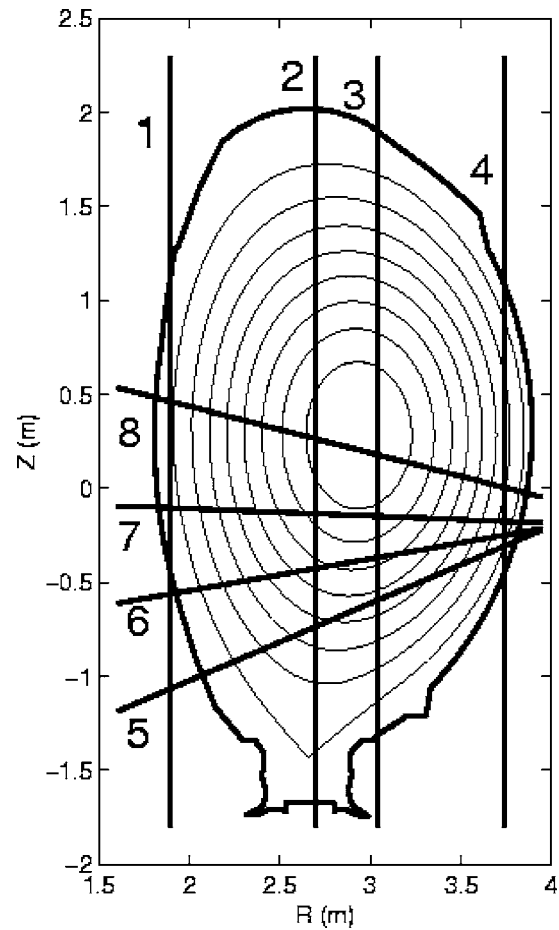


FIG. 1. Lines of sight of the interferometric/polarimetric diagnostic at JET.

Sec. IV). In JET geometry, the Cotton-Mouton effect is proportional to the density times the toroidal field, which is also well known from independent diagnostics. This effect, measured with high accuracy with a particular setup of the diagnostic, does not suffer from the fringe jump problem and can be exploited to correct the vertical channels along which  $B_{\text{tor}}$  is constant.

In the case where many chords are affected by fringe jumps and cannot be recovered, a second approach can be adopted—which consists of estimating the density profile in a simplified way on the basis of the few chords available. In JET, it was demonstrated that the vast majority of line-integrated profiles can be represented by a simple analytical expression, whose parameters can be constrained by the signals of only two interferometric chords; provided one is central and one lateral. The obtained function can then be inverted with help of the Abel integral equation (see Sec. V), providing a density profile of acceptable quality for real-time purposes.

## II. JET INTERFEROMETER/POLARIMETER AND THE PROBLEM OF FRINGE JUMPS

### A. JET Interferometer/Polarimeter

In JET, the interferometer polarimeter was originally conceived to provide the measurements of the plasma density, Faraday rotation, and Cotton-Mouton effects along four

vertical and four nearly horizontal lateral channels (Fig. 1). With regard to the plasma density, the diagnostic implements an interferometer of the Mach-Zehnder type. The relation between the directly measured phase shift and the electron density is expressed by the formula:

$$\Delta\phi = C_{\text{Int}}\lambda \int_1 n_e(l)dl, \quad (1)$$

where  $\lambda$  is the wavelength of the radiation, and  $C_{\text{Int}}$  an appropriate instrumental constant. Given the wavelength used and JET usual densities, the phase difference  $\Delta\phi$  between the reference beam and the one passing through the plasma can very rapidly exceed an angle of  $2\pi$ . Therefore, if in intervals of strong variation of the plasma density the signal is lost, the measurement can be compromised, in the sense that an arbitrary multiple of  $2\pi$  can be spuriously added to the measurements. This kind of error is called a fringe jump because it is normally experienced by the users of the diagnostic as an abrupt and spurious change of the density measurement.

In addition to the interferometric measurements, the use of suitable metallic grids allows the contemporary determination of the polarization state of the beam. Given the geometry of the chords, the Faraday rotation  $\Delta\Psi$  of the beam electric-field polarization plane is linked to the plasma parameters by the relation (first-order approximation):

$$\Delta\Psi = c_{\text{Far}}\lambda^2 \int_1 n_e(l)B_{\parallel}(l)dl, \quad (2)$$

where  $\lambda$  is the wavelength of the radiation,  $c_{\text{Far}}$  is a constant, and  $B_{\parallel}$  is the component of the poloidal field along the direction of the propagation.

The Cotton-Mouton effect in its turn, is expressed by the relation (first-order approximation):

$$\Delta\Gamma = c_{\text{CM}}\lambda^2 \int_1 n_e(l)B_{\perp}^2(l)dl. \quad (3)$$

In Eq. (3) it must be noticed that the change  $\Delta\Gamma$  in the ellipticity of the beam is proportional to the square of the field component perpendicular to the propagation direction of the beam. All mirrors of the vertical channels are installed on an isolated C frame (tower) structure meant to provide enough mechanical isolation. The spurious displacements of the mirrors are therefore normally very low, and for these vertical channels only a Deuterium Cyanide (DCN) laser ( $\lambda=195 \mu\text{m}$ ) was originally foreseen. The lateral channels, on the other hand—as it is often the case in Fusion machines—have to make recourse to in-vessel mirrors to reflect the radiation, and therefore can suffer from large geometrical path variations due to the vibrations of the machines. As a consequence, for these lateral channels, a second alcohol laser ( $\lambda=118.8 \mu\text{m}$ ) is used to implement a compensated interferometer with path length correction (two-color interferometer). The reference beam of both lasers is frequency shifted by a rotating grating to implement a heterodyne detection scheme.<sup>1</sup> The DCN laser is shifted by 100 kHz, whereas the shift of the alcohol laser is only 5 kHz. Both lasers are recombined on the same detectors, and the

separation of the 5 and 100 kHz components is obtained electronically by the use of suitable low-pass (0–30 kHz) and band-pass (60–140 kHz) filters.

With regard to the signal processing electronics, the reference and signal beams are digitized separately at a frequency of 1 MHz, and then resampled with 400 kHz frequency before the phase computation. The polarization measurements, in their turn, are digitized with 1 kHz sampling rate in order to produce data each ms.

## B. The causes of the fringe jump problem

The main reasons behind the vulnerability of JET interferometer to fringe jumps in the phase measurements were carefully investigated first. A detailed analysis of the signals sampled and recorded, at 1 MHz, was performed and the details are reported in Ref. 4. To summarize, the DCN detected signals, in general, drop almost to zero at each fringe jump event. In the case of the alcohol laser, the situation is a bit more involved because in some situations, even if the signal is well above zero, it presents a completely nonperiodic form, indicating the presence of spurious effects. In both situations, it becomes impossible to use the amplitude signal for the calculation of the proper phase difference between the reference and the measuring beam. Since all the cases, during this period of signal loss or deformation, the reference channels do not show any notable amplitude variation, the fringe jumps are attributed to plasma phenomena. In most of the cases, the signal is degraded in the presence of plasma events associated with local density build up (like during ELMs), with a consequent strong increase in the plasma density gradients, or after very fast big changes of the density amplitude (such as, during disruptions or pellets injection). In the first case, the problem is therefore very likely due to refraction; whereas for very fast variations of the density, the main difficulty probably resides in the too slow frequency modulation.

In the following, the various methods implemented at JET to correct the fringe jumps are reported, with particular attention to the assessment of their relative merits and potential of application. For each category of solutions, the technique to detect the occurrence of fringe jumps is introduced first then the correction technique is described together with a short review of the statistical results.

## III. CORRECTION METHODS BASED ON THE INTERFEROMETRIC DATA

### A. Two-color correction method for the lateral channels

Since, as mentioned before, the lateral channels implement a compensated interferometer, the occurrence of fringe jumps can be detected from the time evolution of the path length. Indicating, with  $V$ , the variations of the optical path, the phase measurement of the two wavelengths can be written as follows:

$$\Phi_1 = K\lambda_1 \int_1 n_e dl + \frac{2\pi V}{\lambda_1}, \quad (4a)$$

$$\Phi_2 = K\lambda_2 \int_1 n_e dl + \frac{2\pi V}{\lambda_2}, \quad (4b)$$

where  $\lambda_1$  and  $\lambda_2$  are the main and compensation wavelengths,  $V$  is the change in optical path due to vibrations, and  $K$  is a constant equal to:

$$K = \frac{e^2}{4\pi c^2 \epsilon_0 m_e} = 2.82 \times 10^{-15} [\text{m}]. \quad (5)$$

Multiplying Eqs. (4a) and (4b), respectively, by  $\lambda_1$  and  $\lambda_2$  then making the difference, it is possible to obtain the line-integrated density and vibration amplitude:

$$\int_1 n_e dl = \frac{1}{K} \frac{\lambda_1 \phi_1 - \lambda_2 \phi_2}{\lambda_1^2 - \lambda_2^2}, \quad (6a)$$

$$V = \frac{1}{2\pi} \frac{(\phi_2/\lambda_2 - \phi_1/\lambda_1)}{(1/\lambda_2^2 - 1/\lambda_1^2)}. \quad (6b)$$

This quantity,  $V$ —the variation of the optical path, presents very abrupt changes corresponding when fringe jumps occurs and therefore this measurement can be used to detect them.

Once determined the occurrence of fringe jumps very reliably with the approach discussed above, for their correction a method already devised in Tore Supra<sup>5</sup> was adopted. Since all details of its implementation at JET have already been reported in Ref. 4, in the following, only a concise overview of the technique will be given.

The phase variation between two sampled points—one immediately after the signal is recovered and one just before the fringe jump—can be written in the following way:

$$\Delta\phi_1 + 2\pi\Delta F_1 - \frac{2\pi\Delta V}{\lambda_1} = K\lambda_1 \Delta \int_1 n_e dl, \quad (7a)$$

$$\Delta\phi_2 + 2\pi\Delta F_2 - \frac{2\pi\Delta V}{\lambda_2} = K\lambda_2 \Delta \int_1 n_e dl, \quad (7b)$$

where  $\Delta\Phi$  is the phase variation in the range  $[-2\pi, 2\pi]$ , and  $\Delta F$  is the variation in the number of fringes. By dividing by  $\lambda$  and combining the two equations, it is possible to find the relation:

$$\Delta F_1 = \left( \frac{\Delta\Phi_2}{2\pi} + \Delta F_2 \right) \frac{\lambda_1}{\lambda_2} - \frac{\Delta\Phi_1}{2\pi} - \frac{\Delta V}{\lambda_1} \left[ \left( \frac{\lambda_1}{\lambda_2} \right)^2 - 1 \right], \quad (8)$$

where  $\Delta F_1$  and  $\Delta F_2$ , being fringe jumps, which occur in multiples of  $2\pi$ , must be integer numbers. For long-wavelengths interferometers (typically FIR), on short-time intervals the phase variation due to the change in the optical path,  $\Delta V$ , is usually very small compared to the phase variation due to the density. Neglecting  $\Delta V$  relation (8) gives

$$\Delta F_1 = \left( \frac{\Delta\Phi_2}{2\pi} + \Delta F_2 \right) \frac{\lambda_1}{\lambda_2} - \frac{\Delta\Phi_1}{2\pi}. \quad (9)$$

Various couples of integer values are tried, starting from the lowest numbers, and the one which best satisfies Eq. (9) is chosen, providing the required correction as shown in Fig. 2.

Using the previously described method, in discharges with Type-I ELMs, the density is properly corrected in about

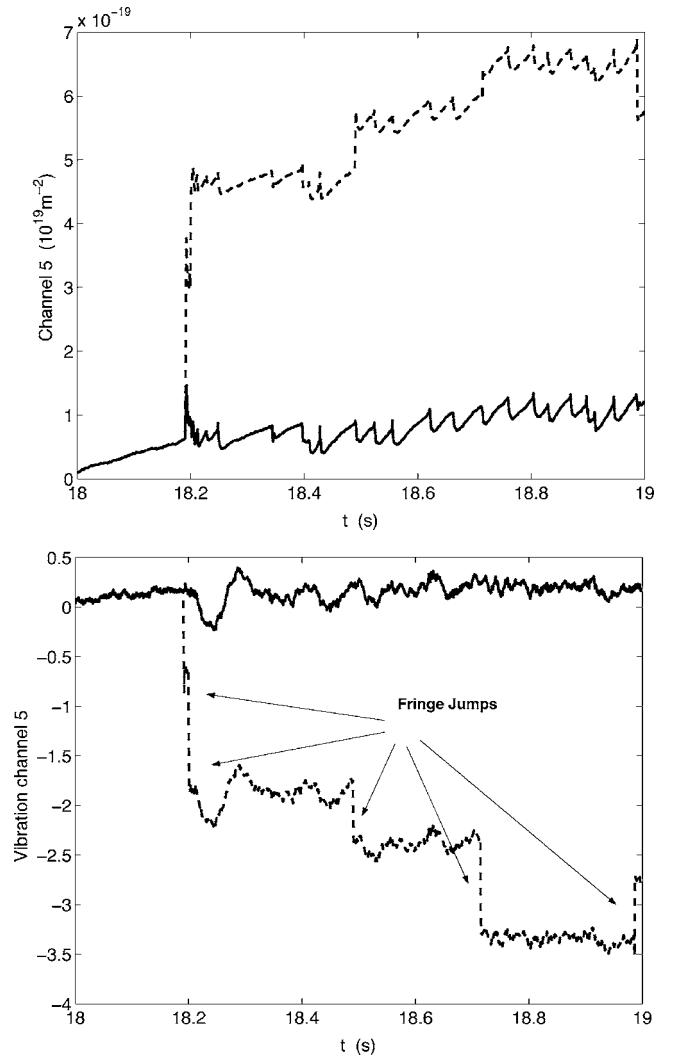


FIG. 2. Comparison between uncorrected (dashed line) and corrected (line) line-integrated density and vibration.

80% of the cases. The statistics is not equally positive in the case of pellets, which are very dramatic events, which can cause the signal being lost for too long to allow a proper correction. For type III ELMs, the situation is more involved and depends on the frequency and strength of the ELMs. To summarize, it can be stated that if the signal can be recovered sufficiently quickly, the percentage of success can be similar to the case of type I ELMs. On the other hand, the performance can deteriorate significantly, with increasing frequency and strength of the events, if the signal is lost for more than 2 ms.

## B. Methods based on interferometric data for the vertical channels

The vertical channels are not compensated (only the DCN laser was installed) and therefore for them a different solution must be found. First of all, an alternative procedure is necessary to identify the occurrence of fringe jumps. This is obtained by comparing the difference between the line-integral density of corresponding vertical and horizontal chords at two consecutive times (chord 2 with 7, chord 3

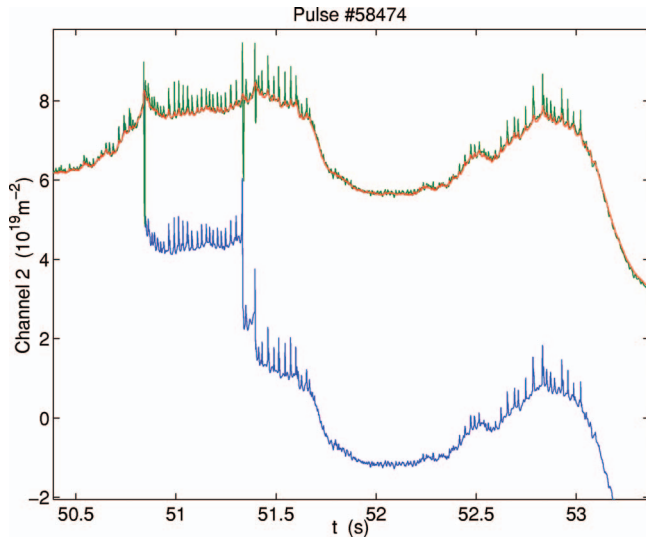


FIG. 3. (Color) Plotting of the uncorrected (blue), reconstructed (red), and corrected (green) densities.

with 8, and chord 4 with 5). Fringe jumps cause this difference to exceed an experimentally found value, revealing their presence.

### 1. Correction based on the density profile

Having detected the fringe jump, a first approach to correct the vertical channels consists of using the whole density profile reconstruction. On the basis of the four lateral channels, possibly recovered with the method described in the previous section, and the correct vertical ones, the density plasma profile is reconstructed, using a best-fit method on the internal magnetic topology, assuming constant density on the iso-flux surfaces.<sup>6</sup> The internal flux surfaces  $f(R, Z)$  are described in the usual parametric form, which depends on elongation, triangularity, and magnetic shift, quantities that can be deduced in real time from the external magnetic measurements:

$$f(R, Z) = \begin{cases} R = R_{\text{axis}} + \Delta(\rho) + \rho \cos[\vartheta + \gamma(\rho)\sin\vartheta] \\ Z = Z_{\text{axis}} + \rho K(\rho)\sin\vartheta, \end{cases} \quad (10)$$

where  $\rho$  is the minor radius of the flux surface,  $\Delta(\rho)$  is the magnetic Shafranov shift,  $\gamma(\rho)$  is the triangularity, and  $K(\rho)$  is the elongation. On the described magnetic topology, interferometric data can then be inverted with a best-fit method and a simple singular value decomposition.

The formula chosen to describe the density profile depends on four parameters ( $n_0, p, q$ , and  $n_w$ ):

$$n_e(\rho) = n_0(1 - \rho^2)(1 + p\rho^2 + q\rho^4) + n_w \quad (11)$$

A careful statistical analysis of many plasma scenarios proves that this parameterization of the density profile is more than adequate for real-time purposes. This is particularly confirmed by a systematic comparison of the derived density profiles with the LIDAR Thomson scattering data.<sup>7</sup> The profiles obtained with this inversion algorithm can be used to calculate the density of the vertical chords affected by fringe jumps. In Fig. 3, the raw signal, the off-line corrected line density, and the output of the correction algorithm are compared, showing the quality of this solution. This

method performs very well in case of fringe jumps due to ELMs and is also quite effective in the case of pellets. In particular, for fringe jumps due to both types I and III ELMs, the recover density measurements increases to a rate of 80%, comparable to the performance of time approach for the horizontal chords. Unfortunately, the elaboration time is of the order of three milliseconds and therefore not always completely satisfactory. In any case, given the typical time scale of JET, this time resolution is more than adequate for the vast majority of real time experiments.

### 2. Correction based on comparison of chords

Since in many applications a faster technique is necessary, a different approach was adopted, based on the direct comparison between vertical and lateral channels, normalized to the length of the line of sight, which is available in JET on a submillisecond time scale.<sup>8</sup> An appropriate geometrical factor, to take into account the plasma shape, is also necessary for the proper application of this approach. Fortunately, this can be in general very easily determined by comparison between the corresponding chords just before the fringe jumps. The “geometrical factor” calculated just before the fringe jump with relations of the kind:

$$\int_{\text{Vertical}} n_e dl = \text{geomFactor} \int_{\text{Lateral}} n_e dl \quad (12)$$

can be used to calculate the number of fringes needed to correct the affected vertical chord:

$$\text{nFringes} = \text{round}\left(\frac{\text{Vertical} - \text{geomFactor} \cdot \text{Lateral}}{1.14 \times 10^{19}}\right). \quad (13)$$

A time resolution of better than one ms is easily achieved with this solution. This method is therefore the one presently implemented at JET. For type I ELMs, the percentage of success is around 60% and for sporadic, individual events good correction can be achieved much more often. An example of successful correction for a discharge with significant ELM activity is shown in Fig. 4, where the density (green) is well recovered after each fringe jump. On the other hand, the main problem is in presence of the high-frequency events, such as type III ELMs, where the corrupted signals are sometimes recovered only after too long and the correction approach fails. So even the success of this technique is strongly dependent on the nature of type III ELMs, and normally fails if the signal is lost for more than 6 ms.

Even if the methods based on purely interferometric measurements are giving positive results and the corresponding algorithms have been implemented and are now routinely used at JET during real-time sessions, they are not completely satisfactory yet. There is therefore some scope in investigating alternative approaches, at least to alleviate the most severe weaknesses of the previous techniques. The first results obtained in trying to exploit the Faraday and the Cotton-Mouton effects are described in the following section.

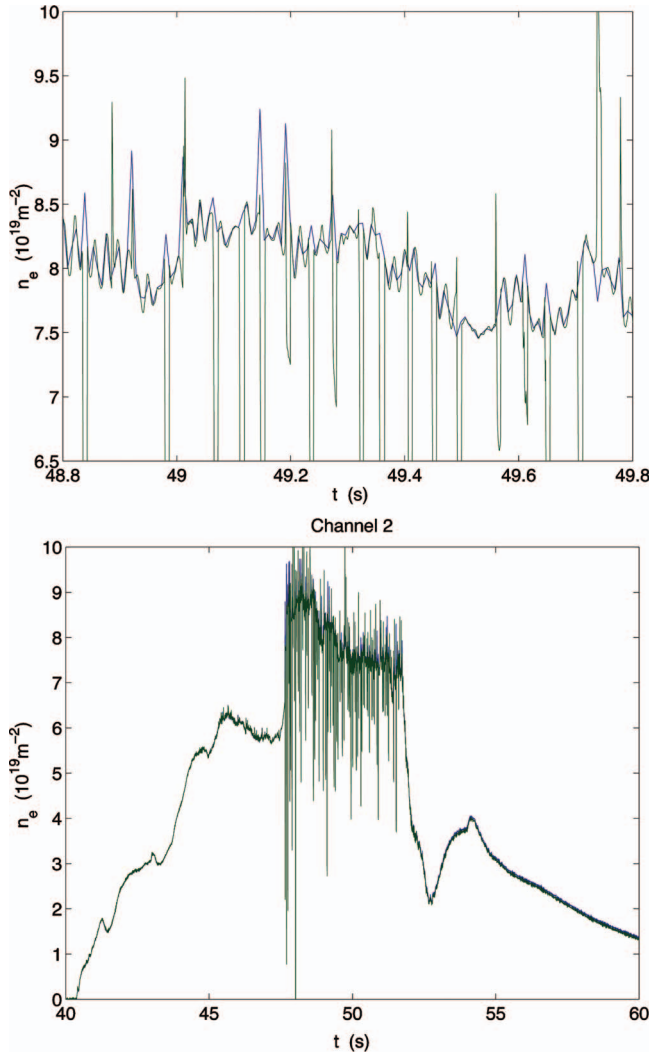


FIG. 4. (Color) Real-time recovered line integral density for channel 2 (green line) compared to the corrected offline density (blue line).

#### IV. CORRECTION METHODS BASED ON THE FARADAY ROTATION AND THE COTTON MOUTON EFFECT

##### A. Technique based on the Faraday rotation effect

As mentioned in the introduction, the Faraday rotation effect consists of a rotation of the polarization plane of linearly polarized radiation, consequence of the optical activity induced in certain media by the presence of a magnetizing field. The relevant component of the field is the one parallel to the direction of propagation. In fusion plasmas, this rotation depends also on the electron density as expressed by relation (2). In JET geometry, the measurement is sensitive according to:

$$\Delta\Psi = c_{\text{Far}} \int_1 n_e(l) B_{\vartheta!!}(l) dl, \quad (14)$$

where  $C_{\text{Far}}$  is a constant and  $B_{\vartheta!!}$  is the poloidal field component along the line of sight. Since the poloidal field ( $B_{\vartheta}$ ) at the edge of a Tokamak can be accurately determined with the help of pick-up coils, whose signals are already available in real time at JET, the Faraday rotation can be used advantageously to correct the most external chords. Indeed, the pre-

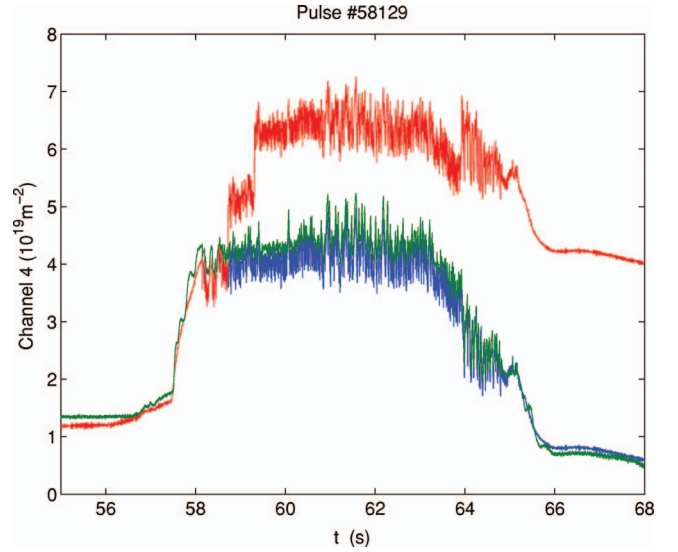


FIG. 5. (Color) Example of the channel 4 correction using Faraday data. (Uncorrected-red, density from Faraday-green, and corrected-blue.)

vious methods for the vertical channels, based on interferometric information only, present a clear weakness in the case of chord four, which, being the most external, has normally a lower signal-to-noise ratio. Assuming constant the poloidal field along the line of sight of chord four, relation (14) gives

$$\Delta\Psi = c_{\text{Far}} B_{\vartheta} \int_1 n_e(l) dl = c_{\text{Far}} B_{\vartheta} N_e \quad (15)$$

from which the line-integrated density can be easily calculated:

$$N_e = c_{\text{Far}} B_{\vartheta} / \Delta\Psi. \quad (16)$$

For the poloidal field, the average of the two values calculated at the intersections between the last close flux surface and the line of sight is generally used.

This alternative estimate of the line-integrated density can be compared with the interferometric data and used to determine the appropriate correction in terms of fringes. The fringe jump detection is completely analogous to the one adopted for the other methods described in the previous section and consists of comparing the line integral of chord 4 with the corresponding measurement of chord 5. An example of correction of chord four with this method based on the Faraday effect is reported in Fig. 5. This approach results particularly useful in discharges in which pellets are launched inside the plasma. In this case, the density rises very fast, with a consequent strong variation of the interferometric measurements, particularly evident in the edge chord 4. The polarimetric data present a much smoother evolution during this fast transient phase, allowing a quite reliable correction even in these situations where the other methods normally fail. On the other hand, since in JET polarimeter the bandwidth of the electronics for the Faraday rotation measurements is much slower than the one of the interferometer, it can be difficult to apply this correction approach to events like the ELMS, which can cause fast oscillations of the edge density.

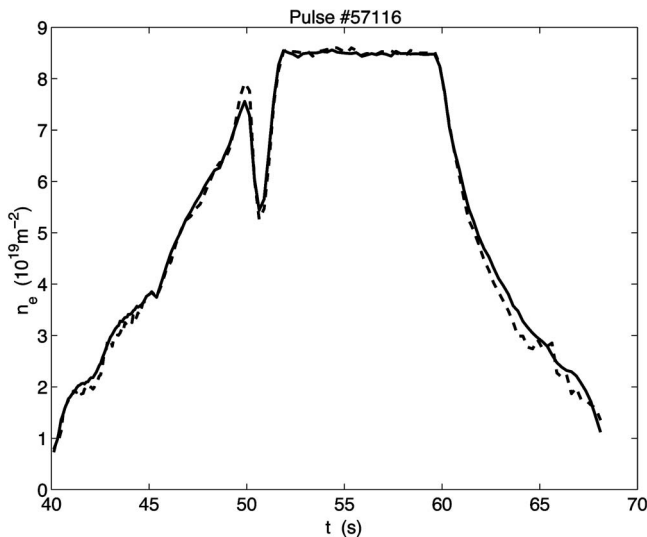


FIG. 6. Line-integrated density for channel 3 measured from interferometry and polarimetry with Cotton-Mouton (dashed line).

### B. Technique based on the Cotton-Mouton effect

The technique based on the Cotton-Mouton<sup>11</sup> effect can be applied only for the vertical channels because the perpendicular field is almost constant along line of sight. As can be seen in relation (3), the polarization depends on the field component perpendicular to the line of sight. In JET geometry as in many other machines, the field perpendicular to the vertical channel is the toroidal field ( $B_\phi$ ) that is well known in Tokamak plasmas. It is worth mentioning that, from a purely theoretical point of view, also a component of the poloidal field should be included into the total perpendicular field but neglecting this term introduces a negligible error.

Since the vertical lines of sight are at fixed radius, it is easy to evaluate the density from the measurements. In a way analogous to the procedure adopted for the approach based on the Faraday effect, the toroidal field, being constant along the beam path, can be extracted from the integral of relation (3):

$$\Delta\Gamma = c\lambda^2 \int_1 n_e(l)B_\phi^2(l)dl = c\lambda^2 B_\phi^2 N_e \quad (17a)$$

$$N_e = c\lambda^2 B_\phi^2 / \Delta\Gamma. \quad (17b)$$

In principal, the method should be very useful for the line integrated density measurements for the vertical channel, as shown in Fig. 6. The line-integrated density obtained with Cotton-Mouton measurements is compared with the interferometric data with good agreement.

Unfortunately at JET the measurement of the Cotton-Mouton effect is not always available, due to spurious oscillations that sometimes jeopardize the signals.<sup>9</sup> In this respect, the diagnostic is not yet reliable enough to be systematically used in real-time control schemes. On the other hand, the approach has been confirmed, since it has proved effective in all cases (100% success), in which the raw data was of acceptable quality. Indeed, if these measurements are of good quality, the Cotton-Mouton effect should be considered more

an alternative way of determining the line integrated density than a correction approach for the interferometer.

### V. ESTIMATE OF THE DENSITY PROFILE WITH THE HELP OF ABEL INVERSION OF ONLY TWO INTERFEROMETRIC CHORDS

The techniques described so far were all aimed at recovering the measurements of the chords affected by the fringe jumps in the best possible way, and introducing the least amount of additional hypotheses. Even if this is not the best attitude from the experimentalist point of view, it must be kept in mind that in many real-time experiments the accurate value of the density is not the main goal. In many cases the density profile can just be instrumental to other quantities or necessary for safety reasons. In these contexts, only a rough estimate of the density profile can be sufficient to proceed with the experiments. On the other hand, if many of the chords are affected by fringe jumps and cannot be recovered, the previously described approaches fail to provide an estimate of the density profile. To overcome this problem and provide an approximate estimate of the density profile, even in cases of many chords being affected by fringe jumps (but having at least two unaffected), the fact that the radial density profile does not vary much in JET can be exploited. Indeed, it turns out that the vast majority of line-integrated density profiles can be represented well by the following expression for line integrated density at a particular radius  $LID(R)$ :

$$LID(R) = C[1 - (1-p)x^2 - px^6], \quad (18)$$

$$x = (R - R_0)/(R_1 - R_0).$$

In Eq. (18),  $R$  is the radial coordinate,  $R_0$  is the position of the maximum of the line-integrated density, and  $R_1$  is the radius of the separatrix. The parameter  $p$  is less than 0.5 for monotonic profiles and higher than 0.5 for hollow ones. Since the geometry can be determined on the basis of the magnetic signals, this analytical function contains only two free parameters (the profile factor  $p$  and the maximum  $C$ ), and can therefore be constrained with the help of only two measurements, provided one is central and one external. At the same the class expressed by Eq. (18) is flexible enough to represent the vast majority of JET density profiles. Assuming that the flux surfaces are concentric ellipses, the function Eq. (18) admits an analytic solution,<sup>10</sup> which can be expressed in the form:

$$n_e(x) = \frac{2C}{\pi(Z - Z_0)} \left[ 1 + 2p - 4p(1 - x^2) + \frac{8}{5}p(1 - x^2)^2 \sqrt{1 - x^2} \right], \quad (19)$$

where  $Z_0$  is the vertical coordinate of the separatrix at  $R_0$ . The category of density profiles described by Eq. (19) is reported in Fig. 7. The obtained solution was compared with the measurements of the Thomson scattering diagnostic, proving that, if constrained by a central and a lateral channel of the interferometer, it provides an estimate of the density profile within an error of about plus minus 20%. The quality



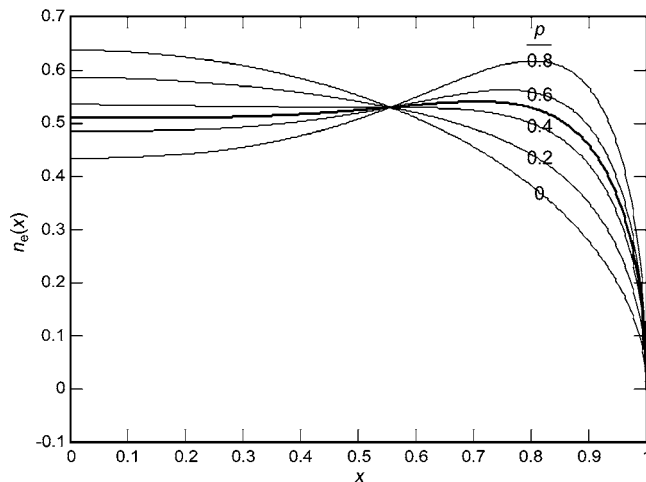


FIG. 7. Class of density profiles represented by relation (19).

of the estimate given by Eq. (19) is shown in Fig. 8 for a JET pulse.

Since the necessary magnetic signals are already available in real time, the implementation of this approach based on relation (19) is straightforward. In terms of elaboration time, the algorithm is very fast and fully compatible with JET real-time system.

## VI. CONCLUSIONS AND FUTURE DEVELOPMENTS

Given the increased interest in feedback experiments at JET, the need for a reliable real-time measurement of the density and related quantities, such as the  $q$  profile, was particularly stringent. This motivated a systematic analysis of the possible approaches for the recovery of the density profile in presence of fringe jumps, which unfortunately affect the JET Interferometer/Polarimeter very often in presence of ELMs or pellets. Two main approaches can be adopted, one to recover the lost signals of the line integrals, the other to estimate the density profile even with a minimum number of only two chords available, provided one central and one lat-

eral. The possible solutions in both categories were tested to determine the pros and cons of the various alternatives. To summarize, it can be stated that the second color is a very important feature and its exploitation provides by far the best results for the lateral channels. For the vertical channels, the solutions using the interferometric data are not completely satisfactory but remain the most reliable for the vast majority of plasma scenarios. In order to improve the rate of success of the correction, for the vertical channels also the available signals of the Faraday rotation and the Cotton-Mouton effect were tested. Unfortunately, the Faraday rotation can be applied reliably only to channel 4 whereas the Cotton-Mouton effect, potentially of higher interest, is at present compromised by the not perfect status of the hardware (a problem not fully understood yet and which will require particular attention in the next campaigns). In any case, a compromise, relying on the second color for the lateral channels and on the chord ratio for the vertical ones, has been implemented and is now systematically used at JET with acceptable performance. The different line of defense, which consists of providing an acceptable estimate of the density profile with a minimum number of correct signals, was also addressed. An analytical expression for the line-integrated density, which can be inverted with the Abel integral in an analytic way, was found. It depends on only two parameters and provides acceptable results provided at least on lateral and one central channel of the interferometer are available.

It is worth mentioning that, irrespective of the detailed implementation to JET, the investigation of the various alternatives is of wider interest, since it could constitute a good guidance to the solution of the same problem in other contexts. The tested solutions, for example, could be implemented in many other fusion devices, since the characteristics of present day interferometers are not too different from one machine to the other.

With regard to future work, given the importance of the information on the density for JET real-time program it is under study for a proposal to implement a second color with shorter wavelength for the vertical channels. This upgrade should provide a complete new independent set of measurements of line integrated density on the vertical system and without presenting fringe jumps. This improvement is due to the fact that the refraction effects will be much smaller at a shorter wavelength, and it will constitute a major step forward in the effectiveness of the correction methods.

Serious consideration is also given to a different approach, meant at investigating whether, with reasonable changes of the hardware, the occurrence of the fringe jumps can be reduced instead of the ability to correct for them once they have happened. It is presently believed, for example, that a faster modulation of the beam and a better phase difference determination by higher sampling rate could have a significant beneficial effect in reducing the number of fringe jumps in the first place.

## ACKNOWLEDGMENTS

The authors would like to thank Klaus Guenther for his pioneering work on the Abel-type inversion of JET density profiles.

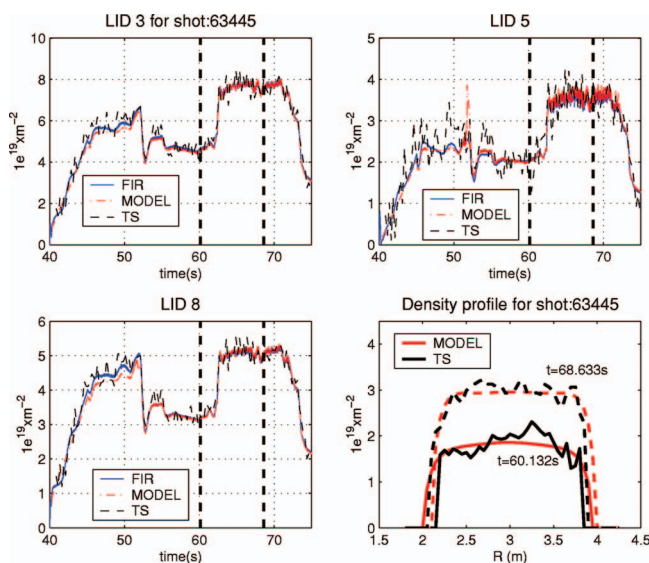


FIG. 8. (Color) Density profiles at different time during a JET pulse.

- <sup>1</sup>I. H. Hutchinson, *Principles of plasma diagnostics* (Cambridge University Press, Cambridge, UK, 2003).
- <sup>2</sup>M. Riva *et al.*, *Proceeding of the 22th Symposium on Fusion Technology (SOFT)* (Helsinki, Finland, 2002).
- <sup>3</sup>G. Braithwaite, N. Gottardi, G. Magyar, J. O'Rourke, and D. Veron, *Rev. Sci. Instrum.* **60**, 2825 (1989).
- <sup>4</sup>P. Innocente, D. Mazon, E. Joffrin, and M. Riva, *Rev. Sci. Instrum.* **74**, 3645 (2003).
- <sup>5</sup>C. Gil, Report Tore Supra, Technical Note No. 97 (CEA Cadarache, France, 1994).
- <sup>6</sup>L. Zabeo, A. Murari, E. Joffrin, D. Mazon, and C. Taliercio, *Nucl. Fusion* **44**, 2483 (2002).
- <sup>7</sup>H. Saltzmann, K. Hirsch, P. Nielsen, C. Gowers, A. Gadd, M. Gadeberg, H. Marmann, and C. Schrodter, *Nucl. Fusion* **27**, 1925 (1987).
- <sup>8</sup>D. O'Brien, J. J. Ellis, and J. Lingertat, *Nucl. Fusion* **33**, 467 (1993).
- <sup>9</sup>D. Elbeze, R. Giannella, C. Gil, and F. Saint-Laurent, *Proceeding of the 30th EPS Conference on Controlled Fusion and Plasma Physics* (2003), p. 4,79.
- <sup>10</sup>K. Guenther, *Fast Analytic Density Profiles Based on KGIV Data and EFIT*, DVCM Internal Report, EFDA-JET, Abingdon, UK, 2004.
- <sup>11</sup>K. Guenther and JET-EFDA Contributors, *Plasma Phys. Controlled Fusion* **46**, 1423 (2004).